Selective Ethanol Synthesis from Carbon Dioxide

ROLES OF RHODIUM CATALYTIC SITES

By Yasuo Izumi

Department of Environmental Chemistry and Engineering, Tokyo Institute of Technology, Yokohama, Japan

Work on the synthesis of ethanol from carbon dioxide over a rhodium-selenium catalyst is reported, and related reactions and characterisation studies are briefly reviewed. In order to inhibit the formation of methane (complete reduction of carbon dioxide) and simultaneously activate carbon-carbon bond formation by the reaction of CH_x with carbonyl derivatives, it is necessary to control the active rhodium sites. Based on a study of single crystal rhodium surfaces it is proposed that acetyl and acetate intermediates are formed. Recently it has been discovered that supported Rh/TiO_2, promoted by selenium from inside the rhodium metal sites, is a potential catalyst for ethanol synthesis from carbon dioxide. The action of this catalyst is compared to related studies.

Emitted carbon dioxide has been implicated as one of the major sources of global warming. Therefore the conversion of carbon dioxide into alcohols is an environmentally desirable process, making use of an abundant, cheap resource.

The synthesis of methanol from synthesis gas $(CO + H_2)$ is a well known process (1–3). The dissociation energy for carbon monoxide is large $(1071.8 \text{ kJ mol}^{-1})$. It chemisorbs on metal surfaces via the carbon atom through the 5σ orbital, which is the HOMO (highest occupied molecular orbital). When adsorbed CO, CO(ads), is completely hydrogenated, the product will either be methanol or methane, depending on whether the C-O bond is retained or cleaved, respectively.

The C-O dissociation energy for carbon dioxide $(526.1 \text{ kJ mol}^{-1})$ is smaller than for carbon monoxide. The HOMO, $1\pi_g$, is on the two oxygen atoms, which suggests that the reactions of carbon dioxide occur in a direction perpendicular to the O-C-O bond. Due to these bonding differences, carbon dioxide can undergo a much wider range of chemical transformations on a heterogeneous catalyst surface. For example, protonation forms formate species,

$HCO_2(ads)$, while reaction with a surface hydroxyl group or oxygen should produce carbonate species, $CO_3(ads)$. Cleavage of one of the C-O bonds often occurs on a transition metal surface, making the reaction more complex, due to the formation of CO as an intermediate species. (In this case the selectivity reflects the reaction path.)

Under reducing conditions, methane and lower hydrocarbons $(2 \leq C \leq \approx 10)$ are predominantly produced from $CO_2 + H_2$ on most platinum group metal catalysts, and here we examine some studies for controlling the conversion of carbon dioxide to ethanol. In relation to our new $Rh_{10}Se$ catalyst, a proposed reaction intermediate, which forms during ethanol synthesis, is described, and the controlled reaction path over our new ethanol synthesis catalyst is reported. The structure and electronic state of the rhodium catalyst sites are studied.

Proposed Mechanism Based on an Acetate Intermediate

Model studies of ethanol decomposition and oxidation on Rh(110) have been reviewed (4). Stable acetate species are formed on the surface

Scheme
The stabilisations of:
(a) acyl species by adsorbed oxygen and
(b) propanoyl species by promoter selenium
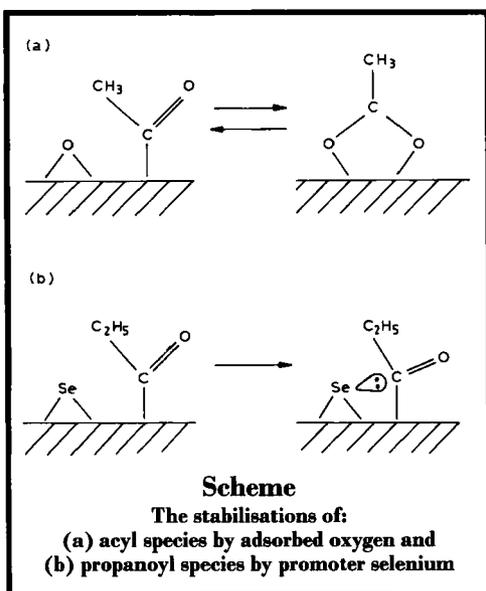
of pure rhodium. Acyl species, formed from the decomposition of adsorbed ethanol, interact with surface oxygen atoms to form the more stable acetate, see Scheme (a). Indeed, it has been proposed that the role of promoters, which preferably exist as metal oxides, is to effect this stabilisation of acetyl species (evident in temperature programmed desorption) by forming surface acetates.

Findings similar to this study of a model rhodium surface have been reported for selenium-doped Rh/ZrO$_2$ (5) and Rh/SiO$_2$ catalysts (6). During ethene hydroformylation (C$_2$H$_4$ + CO + H$_2$) propanoyl species (C$_2$H$_5$CO) were detected predominantly on rhodium metal sites, by FT-IR (Fourier Transform Infrared) spectroscopy, at 1770 and 1740 cm^{-1} for Se-Rh/ZrO$_2$ and Se-Rh/SiO$_2$, respectively. Propanoyl, corresponding to the acetyl species formed from ethanol decomposition on the Rh(110) surface, was formed by the migration of C$_2$H$_5$(ads) to CO(ads). The doped selenium had an electrical charge of –2 and ~ –1 for Se-Rh/ZrO$_2$ and Se-Rh/SiO$_2$, respectively, and is suggested to function as a base to stabilise the propanoyl intermediate by "locking" the carbonyl carbon, see Scheme (b) (based on temperature-programmed desorption and *in-situ* FT-IR studies

(5)). Propionate species formed from the reaction of propanoyl with O(ads) were also detected on these catalysts; however, they were mainly stabilised on the surface of the support, and were in equilibrium with propanoyl species on the rhodium surface.

Lithium or Iron-Promoted Rh/SiO$_2$ Catalysts

Extensive surveys of carbon dioxide hydrogenation have been reported on promoted Rh/SiO$_2$ catalysts (7, 8). On unpromoted Rh/SiO$_2$ methane was the major product. Among promoter atoms that have been examined, it was found that co-impregnation with lithium, strontium, iron and silver promoted ethanol formation (7). With lithium, ethanol selectivity was 15.5 per cent at 5 MPa and 513 K, and with iron (at a molar ratio iron:rhodium = 2) the ethanol selectivity was 16.0 per cent at 5 MPa and 533 K (8).

Poisoning and Promotion Effects of Selenium from Inside Rh$_{10}$ Cluster Sites

As described above, in general, supported rhodium metal sites easily dissociate the C–O bonds of CO$_2$ leading to the formation of methane and lower hydrocarbons. For example, when the iron:rhodium ratio was varied in iron-promoted Rh/SiO$_2$, the selectivity and conversion into ethanol reached a maximum around iron:rhodium = 2 (8). (The dependence of selectivity and conversion is often observed having a maximum as a function of the amount of promoter.) However, the reason for the dependence is not completely clear because an excessive amount of doping by promoter can affect the result by steric (geometric) poisoning and/or by electronic induction, and it is hard to distinguish between the two.

The synthesis of ethanol from carbon dioxide and hydrogen over [Rh$_{10}$Se]/TiO$_2$ is examined in the Table (9). At the lower temperature (523 K), the initial rate of formation of ethanol was 1.9 × 10^{-3} mol h^{-1}g$_{cat}^{-1}$ and the selectivity to ethanol was 83 per cent. The synthesis rate increased with reaction temperature, to reach 6.0 × 10^{-3} mol h^{-1}g$_{cat}^{-1}$ at 723 K. However, the

Ethanol Synthesis on Supported [Rh₁₀Se] and Conventional Rh/TiO₂* Catalysts				
(A) Using carbon dioxide and hydrogen				
Catalyst	T_{react}, K	Initial rate, 10^{-3} mol h^{-1}g$_{cat}^{-1}$		Ethanol selectivity, mol %
		Ethanol	Methane + CO	Ethane	
[Rh₁₀Se]/TiO₂	523	1.9	0.4	0	83
	623	3.7	1.4	0	71
	723	6.0	5.8	0	51
[Rh₁₀Se]/Al₂O₃	623	0	0.15	0	0
[Rh₁₀Se]/MgO	623	0	0.04	0	0
[Rh₁₀Se]/SiO₂	623	0	0	0	0
[Rh₆C]/TiO₂	623	0.4	1.2	2.4	10
[Rh₆]/TiO₂	623	0	6.2	0	0
Rh/TiO₂	623	0	1.8	0	0
(B) Using carbon monoxide and hydrogen				
Catalyst	T_{react}, K	Initial rate, 10^{-3} mol h^{-1}g$_{cat}^{-1}$		Ethanol selectivity, mol %
		Ethanol	Ethane	
[Rh₁₀Se]/TiO₂	623	0	0.03	0

Total pressure 47 kPa; P_{CO_2} (or P_{CO}) : P_{H_2} = 1 : 2; Rh 1.3 for TiO₂ and Al₂O₃, 2.8 for SiO₂ and 1.6 wt.% for MgO.
* As pretreatment, incipient catalyst was in vacuum at 593–673 K, then in hydrogen at 623 K for 1 h.
Rh/TiO₂ was in vacuum at 523 K, then in O₂/H₂ at 523 K

selectivity gradually decreased with increasing reaction temperature due to the larger activation energy for methane + CO.

The model catalyst was prepared from the organometallic cluster $[Rh_{10}Se(CO)_{22}]^{2-}$ and the starting supported catalyst was totally decarbonylated by heating in vacuum (9–12). The structure of the active sites was studied by EXAFS (Extended X-ray Absorption Fine Structure) spectroscopy, which is tunable to the absorption edge of each element. Both selenium K- and rhodium K-edge EXAFS spectra were measured for [Rh₁₀Se]/TiO₂ catalyst (12). By curve fitting analysis of selenium K-edge EXAFS, based on model EXAFS parameters of $[Rh_3Se_2(CO)_6]^-$ (Se-Rh bond) and SeO₂ (Se-O bond), the Se-Rh bond distance was found to be 2.41 Å. The fit was dramatically improved by two-wave fitting, suggesting the existence of a surface oxygen atom at a distance of 1.97 Å from selenium. The model parameters for rhodium K-edge curve fitting were extracted from rhodium foil (Rh-Rh bond), Rh₃Se₈ (Rh-

Se bond) and Rh₂O₃ (Rh-O bond). The best fit for rhodium K-edge EXAFS showed the bonding distances for Rh-Rh, Rh-Se and Rh-O to be 2.72, 2.41 and 2.09 Å, with co-ordination numbers 4.0, 1.0 and 1.5, respectively. In comparison with $[Rh_{10}Se(CO)_{22}]^{2-}$ (4.8), the co-ordination number, N_{Rh-Rh} (4.0) became smaller, due to partial decomposition of the [Rh₁₀Se] core by the formation of Rh-O(surf) bonds.

Based on all the bond distances and co-ordination numbers obtained by EXAFS, a surface cluster model in which four rhodium atoms are interacting with O(surf) of TiO₂ was proposed (12).

It is interesting to compare this model cluster consisting of ten rhodium atoms and one selenium atom (atomic ratio Se:Rh = 0.1) to other reports. When dimethyl selenide (gas) was reacted with [Rh₆]/MgO, prepared from Rh₆(CO)₁₆, the ethene hydroformylation reaction rate to propanal + propanol reached a maximum at around Se:[Rh₆] = 0.6 (10). The atomic Se:Rh ratio was 0.1, equivalent to that for

[$Rh_{10}Se$]/TiO_2. However, this may be coincidental, due to the complex effects of the selenium promoter. When the amount of selenium increased to the ratio Se:[Rh_6] = 2, the selenium-doped [Rh_6]/MgO lost all its catalytic activity. It appears that geometric hindrance of the reactants was significantly affected by poisoning of [Rh_6]/MgO (doped onto the rhodium surface). Selenium in the [Rh_{10}] framework should affect the poisoning only electronically.

Different supported rhodium clusters have been prepared and compared with [$Rh_{10}Se$] for the CO_2 + H_2 reaction, see the Table (9). The [Rh_6]/TiO_2 was the most active, but only produced methane and/or CO. Rh/TiO_2, prepared by conventional impregnation from the Rh salt, also only formed methane + CO, but at a lower rate resulting from the larger rhodium particle size, as observed by EXAFS. [Rh_6C]/TiO_2 gave ethanol, but significant amounts of methane (+ CO) and ethane were also produced, suggesting that inhibition of the total carbon dioxide reduction was not as successful on [Rh_6C]/TiO_2 (ethanol selectivity was 10 per cent) compared to [$Rh_{10}Se$]/TiO_2 (71 per cent). Special features of using [$Rh_{10}Se$] for ethanol synthesis should be the retention of the [$Rh_{10}Se$] cluster under the reaction conditions (stabilisation by selenium) and an effective electronic modification by selenium (anionic selenium contacts all the ten rhodium atoms in the cluster).

Reaction Mechanism of Ethanol Synthesis on [$Rh_{10}Se$]/TiO_2 Catalyst

The reaction mechanism for the formation of ethanol from CO_2 + H_2 on [$Rh_{10}Se$]/TiO_2 was studied by *in-situ* FT-IR (11). The intensity of two peaks (1614 and 1243 cm^{-1}) increased during the course of the reaction. They were assigned to bidentate carbonate species, based on the frequencies for [$Co(NH_3)_4(CO_3)$]$^+$ (1635–1593 and 1292–1265 cm^{-1}) (13). Two peaks were observed in the same region (1570 and 1230 cm^{-1}) for unimpregnated TiO_2 in CO_2 + H_2. Two unresolved peaks between the two carbonate peaks were also measured. On the basis of several references in (4), these two peaks may be assigned to acetate species. The

carbonate species on the [$Rh_{10}Se$]/TiO_2 should be affected by the [$Rh_{10}Se$] cluster, as they are either near the [$Rh_{10}Se$] or on the Rh of [$Rh_{10}Se$]. A peak at 3356 cm^{-1} was also observed for unimpregnated TiO_2 which shifted to 2460 cm^{-1} in deuterium gas, showing that the peak was due to hydroxyl species on TiO_2.

The increases in intensity of the peaks at 2965, 2883, 2919 and 2853 cm^{-1} were proportional to the ethanol synthesis rates, and were assigned to CH_3 v_{as}, v_s, CH_2 v_{as}, and v_s, respectively. The dissociation of the C-O bonds of carbon dioxide occurred on rhodium and the four peaks rapidly disappeared when the supply of reaction gas (CO_2 + H_2) was discontinued. This suggests that the methyl and methylene species are formed mainly on rhodium. The intensities of the CO stretching peaks (2174 and 2108 cm^{-1}) were weak compared to those for [$Rh_{10}Se$] supported on Al_2O_3, MgO and SiO_2, which exhibited lower total activities and no activities to ethanol.

The reason why CO(ads) was not stabilised on [$Rh_{10}Se$]/TiO_2 is unclear, but the different co-ordination number around rhodium, compared with that around conventional rhodium or supported [$Rh_{10}Se$]/Al_2O_3, [$Rh_{10}Se$]/SiO_2 or [$Rh_{10}Se$]/MgO catalysts, may be important (12). These two wavenumbers, 2174 and 2108 cm^{-1}, were relatively high, suggesting that CO was bound to relatively positive rhodium sites.

Based on these assignments and on the peak intensity changes, a mechanism for ethanol synthesis on [$Rh_{10}Se$]/TiO_2 is proposed, see Figure 1. The CH_3(ads) or CH_2(ads) on rhodium may first react with CO_3(ads) or CO_2, followed by hydrogenation to ethanol on the rhodium sites. The reaction of CO + H_2 was very slow and totally different from the reaction of CO_2 + H_2 on [$Rh_{10}Se$]/TiO_2, suggesting that ethanol synthesis does not proceed via CO for this catalyst.

On many rhodium catalysts, the order of reaction with respect to CO is negative, thus high CO concentrations would poison the reaction. Hence, it is possible in this case that CO_2 provides a small, steady state amount of CO for this reaction (14). The observed acetate species may support the reaction mechanism, *not* via CO as

Fig. 1 The proposed reaction mechanism of ethanol synthesis from $CO_2 + H_2$ on $[Rh_{10}Se]/TiO_2$ catalyst. The reaction between $CO(ads)$ and $CH_x(ads)$ to form ethanol is also possible
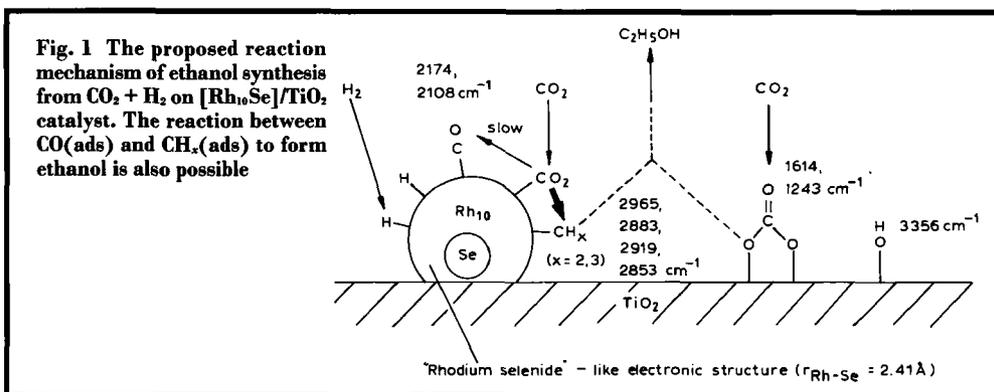
shown in Figure 1. The stability of the $CH_x(ads)$ on rhodium should be a key point, the rhodium site being affected by the interior negatively charged selenium ($-1 \sim -2$ by XPS) (12). The "rhodium selenide"-like electronic state inhibited methane formation, but tuned the reaction path to ethanol by promoting the C-C bond formation of CH_x with the carbonyl derivative.

Summary

Controlling the reaction path of $CO_2 + H_2$ to give ethanol was found to be possible due to the presence of carbon, oxygen, selenium, lithium and iron around rhodium sites. Electronic control by selenium for ethanol formation was investigated by several techniques, and electronic modification of the platinum metal cluster from within should be applicable to other systems.

References

1 E. L. Muetterties and M. J. Krause, Angew. Chem., Int. Ed. Engl., 1983, 22, 135

2 E. L. Muetterties and J. Stein, Chem. Rev., 1979, 79, 479

3 K. Klier, Adv. Catal., 1982, 31, 243

4 M. Bowker, Catal. Today, 1992, 15, 77

5 Y. Izumi, K. Asakura and Y. Iwasawa, J. Catal., 1991, 127, 631

6 Y. Izumi, K. Asakura and Y. Iwasawa, J. Catal., 1991, 132, 566

7 H. Kusama, K. Sakama, K. Okabe and H. Arakawa, Nippon Kagaku Kaishi, 1995, 875

8 H. Kusama, K. Okabe, K. Sakama and H. Arakawa, Energy, 1997, 22, 343

9 H. Kurakata, Y. Izumi and K. Aika, Chem. Commun., 1996, 389

10 Y. Izumi and Y. Iwasawa, J. Phys. Chem., 1992, 96, 10942

11 Y. Izumi, H. Kurakata and K. Aika, Hyomen-Kagaku (Surface Science), 1996, 17, 242

12 Y. Izumi, H. Kurakata and K. Aika, submitted to J. Catal.

13 K. Nakamoto, "Infrared and Raman Spectra of Inorganic and Coordination Compounds", Third Ed., John Wiley & Sons, New York, 1970

14 For example, (a) J. S. Lee, K. H. Lee, S. Y. Lee and Y. G. Kim, J. Catal., 1993, 144, 414; (b) R. A. Koeppel, A. Baiker and A. Wokaum, Appl. Catal. A, 1992, 84, 77

Hexagonal Nanostructured Platinum

Platinum particles can be prepared as nanostructures or monolayers, in polymers and in templates of ceramic materials by the reduction of platinum acids or salts. Researchers from the U.K. and Germany now report the use of a liquid-crystalline phase template to form nanostructured platinum (G. S Attard, C. G. Göltner, J. M. Corker, S. Henke and R. H. Templer, Angew. Chem. Int. Ed. Engl., 1997, 36, (12), 1315–1317).

Hexachloroplatinic acid and ammonium tetrachloroplatinate were added to the surfactant, octaethyleneglycol monohexadecyl ether, which was used to prepare the lyotropic liquid-crystalline phases because it forms a wide hexagonal mesophase. The platinum salts were reduced, forming platinum powder of particle size 90 to 500 nm of hexagonal nanostructure with cylindrical pores 30 Å in diameter, separated by 30 Å thick platinum walls. The lyotropic phase may act as a structure-directing medium. Platinum is stabilised at the hydrophobic/hydrophilic interface as small colloidal particles which agglomerate and coalesce to a stable wall thickness. Only fast reductions allow this structure to form before the liquid-crystal phase rearranges.

This nanostructured platinum is mesoporous and of large surface area – features useful for catalytic, fuel cell and sensor applications.